

EARLY BRONZE AGE CHRONOLOGY: RADIOCARBON DATES AND CHRONOLOGICAL MODELS FROM TEL YARMUTH (ISRAEL)

Johanna Regev^{1,2} • Pierre de Miroschedji³ • Elisabetta Boaretto²

ABSTRACT. Over the years, 40 radiocarbon samples (charcoal and seeds) have been measured from the site of Tel Yarmuth. These samples originate from 3 major archaeological periods: Final Early Bronze Age (henceforth EB) I, EB II, and EB IIIB-C. The samples are further on divided into 8 separate archaeological phases. Bayesian modeling analyses were performed on the data. Separate models were run with seeds and charcoals to detect a possible old-wood effect. Outliers were detected, and finally models with gaps were run to account for the lack of samples from 2 archaeological layers. The results suggest that at Tel Yarmuth the end of the EB II occurred ~2950–2880 BC, and that the EB III ended *at the latest* ~2450 BC, perhaps before 2500 BC. Although these dates are somewhat earlier than traditionally assumed, they are in close accordance with the new analysis of other ¹⁴C dates for the Early Bronze Age in the southern Levant (Regev et al., these proceedings).

INTRODUCTION

The absolute chronology of the Early Bronze Age of the southern Levant is based on comparisons between pottery types securely placed within the local pottery sequence and comparable pottery types found in Egypt in historically dated contexts (Hennessy 1967; Ben-Tor 1991; Sowada 2009). A relative chronology has thus emerged, accepted by most scholars (e.g. Ben-Tor 1992; Mazar 1990; de Miroschedji 1999, in press a). It suggests that the Final EB IB period dates to the very end of the 4th millennium BC in Egypt (van den Brink and Levy 2002), while the EB II period is more or less synchronous with the first 2 dynasties, dated ~3000–2700 BC in the consensual “high” chronology (Kitchen 1991; Shaw 2000), and the EB III period with the Old Kingdom (dynasties 3 to 6), dated about 2700–2200 (Kitchen 1991; Shaw 2000). Other chronologies exist, which lower by 1 century or more the beginning of the 1st Dynasty (e.g. Hornung et al. 2006; Jiménez Serrano 2007; Wenke 2009). A chronology based on radiocarbon dates has recently been proposed by Bronk Ramsey et al. (2010). For the first half of the 3rd millennium, the latter chronology modifies only marginally the consensual High Chronology. As for the end of the EB III, it is conventionally placed around 2350–2300 BC, i.e. during the 6th Dynasty in Egypt (Mazar 1990; de Miroschedji 1999, in press b).

The basis for this absolute chronology is thus strictly historical and depends on the validity of the reconstruction of the Egyptian king lists and reign lengths inferred from written and archaeological sources. Given the uncertainty surrounding this historical chronology, the establishment of a calibrated ¹⁴C timescale is the only way to build on an independent basis the absolute chronology of the southern Levant.

Among the major Early Bronze Age sites of the southern Levant, Tel Yarmuth ranks prominently because of its size (16 ha), the large exposures of the Early Bronze Age strata exhibiting monumental architectural remains, the length of its stratigraphic record, and its many ¹⁴C samples recovered from well-defined stratigraphic contexts. Tel Yarmuth is thus an excellent site to carry out a detailed ¹⁴C study of the Early Bronze Age with the aim of laying the ground for an absolute chronology.

¹The Martin (Szusz) Department of Land of Israel Studies and Archaeology, Bar Ilan University, 52900 Ramat Gan, Israel. Corresponding author. Email: johanna.regev@gmail.com.

²Radiocarbon Dating and Cosmogenic Isotopes Laboratory, Kimmel Center of Archaeological Science, Weizmann Institute of Science, 76100 Rehovot, Israel.

³UMR 7041 (HAROC) - Archéologies et Sciences de l'Antiquité, Maison de l'archéologie et de l'ethnologie, Boîte 17, 21, allée de l'Université, 92023 Nanterre cédex, France.

RADIOCARBON SAMPLES: PROVENANCE

The Site and Its Stratigraphy

Tel Yarmuth is located 25 km southwest of Jerusalem (Figure 1). Nineteen seasons of excavations have been conducted at the site, one under the direction of A Ben-Tor in 1970 (Ben-Tor 1975), and 18 under the direction of P de Miroschedji since 1980 (see de Miroschedji et al. 1988; de Miroschedji 1999, 2003, 2008). Altogether, 13 areas of excavations (A-N) have been opened in the Lower City (Figure 2), some subdivided into several subareas (e.g. Area Ja to Jc).

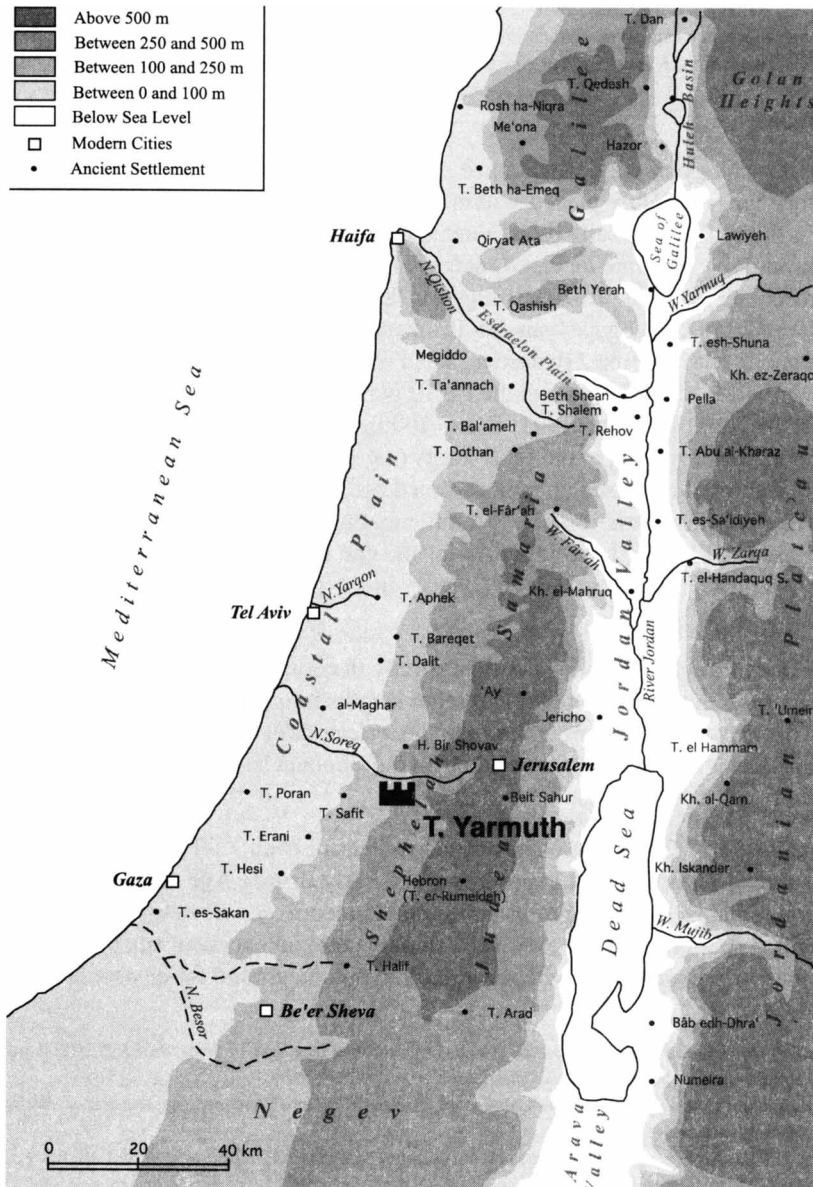


Figure 1 Map showing the location of Tel Yarmuth

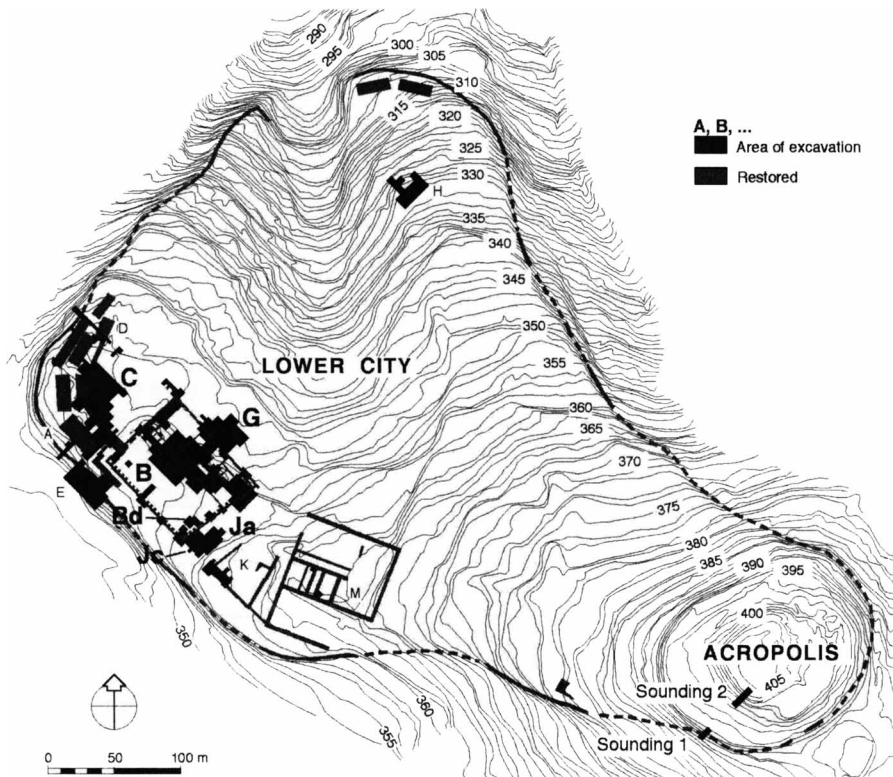


Figure 2 Plan showing the location of the excavation areas at Tel Yarmuth. The bold letters indicate the areas from which ^{14}C samples discussed in this paper originate.

These excavations have revealed a long sequence of occupation, stretching from the Early Bronze IB (the so-called “Erani C Phase,” ~3300 BC in the conventional chronology) to the very end of the EB III (EB IIIC phase, ~2350/2300 BC in the conventional chronology), represented by large-scale public and private architecture (including 2 successive palaces, a temple, 5 areas of domestic dwellings, and a possible oil factory), powerful fortifications (2 city walls, 8 bastions, 3 city gates), and a system of urban terracing.

The stratigraphic correlations between these excavation areas are based on similarities of archaeological material, mainly pottery, and/or on the relative stratigraphic position of the strata in relation to an architectural feature encompassing different areas, such as City Wall A or Palace B1.

Contexts of the Samples

The ^{14}C samples were collected during excavation, either directly by hand when they could be easily spotted or (in the case of seeds) after flotation of sediment samples. A few additional samples (e.g. RTT-5902 to -5905) were collected *ad hoc* by E Boaretto and J Regev in 2006 after cleaning of stratigraphic sections and identification of clusters of seeds in controlled stratigraphic contexts. Although a large number of samples were collected, only 40 of them were selected for dating on the basis of the nature and quality of their archaeological context: only samples found on floors or in sealed contexts were used. The areas from which these samples originate are shown in bold letters in Figure 2 and their stratigraphic distribution is given in Table 1. Table 1 provides information on

the stratigraphic and archaeological provenience of the 40 samples, and are arranged by area, in chronological order from the most ancient to the most recent archaeological contexts.

Table 1 Stratigraphic distribution of the ¹⁴C samples of Tel Yarmuth. A vertical line between 2 numbers indicates that the samples were in direct superposition, a horizontal line that they come from the same layer. The numbers within a box correspond to samples retrieved from the same stratigraphic context, although not always in close proximity.

| Period | Area - Stratum | | | | | | |
|-----------------------|--|---------------------|---------------------|----------------------------|----------------------|--------------|---|
| | C-9 to C-6 | Jc-Phase 3 | Bd-2 | Ja-3 | G-3 | B-2 | B-1 |
| C EB III B A | | | | | | 5295 5296 | 2964 2965 2966 2967 2968 3495 5293 5294 (2963) (2969) |
| | | | | 5286 5283 — 5285 | 3505 3506 3508 | | |
| | | | 3493 | | | | |
| | Hiatus corresponding to Strata C-5 to C-3 (early part of EB III) | | | | | | |
| EB II | C-6 | 3502 | 5288 5289 — 5290 | | | | |
| | C-7 | 3496 5292 — 3497 | 3501 | | | | |
| | C-8 | 5903 5902 | 3498 | 3503 — 3500 3504 — 5291 | | | |
| EB IB Final | C-9 | 5904 — 5905 | 3499 | | | | |

Area C (15 Samples)

Located in the west corner of the city, Area C covered 950 m² and revealed 9 strata (C-9 to C-1, from bottom to top). Stratum C-9, exposed in small probes only, consists of a thin layer (~0.20 m) with occupation surfaces resting directly on bedrock and no associated architecture. The archaeological material is ascribed to the very end of the EB I period (Late EB IB). Sporadic finds of sherds dating to the EB IB [Erani C Phase] attest to an earlier occupation of the site but they were not found in clear stratigraphic context and have not yielded datable ¹⁴C samples. This stratum yielded 2 samples of seeds (RTT-5904 and -5905). Stratum C-8 was also excavated in small soundings only and dates to the very beginning of the EB II. It belongs to an apparently unfortified settlement with some significant architectural remains. Seven samples originate from this stratum (RTA-3498, -3500, -3503, -3504; RTT-5291, -5902, -5903). The latter 3 samples were collected just beneath the foundation of City Wall A). One other sample (RTA-3499) comes from a context that may belong either to Stratum C-9 or C-8. The following strata C-7 and C-6 date to the traditional EB II period. Stratum C-7 is contemporaneous with the construction and early use of City Wall A. It has yielded 4 samples (RTA-3496, -3497, -3501; RTT-5292). Only 1 sample (RTA-3502) comes from Stratum C-6. The uppermost strata, C-5 to C-1, all belong to the EB IIIA-B and have not yielded any samples appropriate for ¹⁴C dating.

Subarea Jc (3 Samples)

Subarea Jc corresponds to the part of Area J located outside (i.e. southwest) of City Wall A, which marks the limit of the first EB II settlement. A deep probe was excavated there through a fill intentionally deposited between City Wall A and City Wall B. This fill is ascribed to the second phase of the fortification system dated to a later part of the EB II (see de Miroschedji et al. 1988). The 3 samples (RTT-5288 to -5290) originate from layers of ashy sediments sealed by plastered surfaces in the upper part of the fill. The pottery assemblage suggests that they are contemporaneous with Stratum C-6 within the settlement.

Subarea Bd (1 Sample)

Subarea Bd is located along the southeast side of the main courtyard of Palace B1 and covers an area of 150 m². Three strata were identified (Bd-3 to Bd-1), all dated to the EB III period. Stratum Bd-1 corresponds to Palace B1 (Stratum B-1), while Stratum Bd-2 (from which sample RTA 3493 was obtained) is contemporaneous with strata B-3 or B-4.

Area G (4 Samples)

Area G is situated to the southeast of Area C and extends along part of the northeastern side of Palace B1. It was excavated over 500 m² and revealed 6 strata (G-6 to G-1) partly synchronous with those of Area B. Three samples (RTA-3505, -3506, -3508) originate from Stratum G-3, which is the extension of Stratum B-3 to the northeast of Area B. Stratum G-3 is represented by a series of domestic dwellings in which complete vessels were found *in situ* on floors. In its southwestern part, this stratum was violently destroyed, together with strata B-3, J-3, and K-2, prior to the construction of Palace B2. A fourth sample (RTA-3507) from Stratum G-2 unexpectedly provided a “very old” date (see Table 1) and had to be discarded.

Subarea Ja (5 Samples)

Subarea Ja occupies a low terrace alongside the southeastern wall of Palace B1 and is limited to the southwest by the line of City Wall A. Partial excavations revealed 4 strata, J-1 to J-4 (from top to bottom). Strata J-1 and J-2 correspond, respectively, to strata B-1 and B-2. Stratum J-3 is coeval with Stratum B-3 and was also violently destroyed. Five samples (RTT-5283 to -5287) were retrieved from the destruction layer among vessels crushed on the floor under the fallen roof. Two of these samples (RTT-5284 and -5287), however, unexpectedly provided a post-bomb (i.e. modern) date and were clearly intrusive.

Area B (12 Samples)

The extent of Area B is defined by the limits of Palace B1. The stratigraphic sequence comprises 6 strata, B-1 to B-6, from top to bottom (de Miroschedji et al. 1988:31–3). Extensive excavations were carried out only for strata B-1 (= Palace B1), B-2 (= Palace B2), and B-3. The latter is equivalent to strata G-3 and J-3. Stratum B-2 corresponds to the first palace erected on the leveled ruins of a violently destroyed area. Since this palace was razed to the ground to be replaced by Palace B1, few floors were preserved. Two samples of seeds (RTT-5295, -5296) were nevertheless collected from a sound context (L.2632) sealed by a floor of the overlying Stratum B-1. The latter stratum yielded 8 samples (6 charcoals, 2 seeds) all retrieved from floors of Palace B-1, together with a large amount of complete vessels. Two additional samples from this stratum deserve a special note: RTT-2969 is a fragment of charcoal from a wooden post resting on a stone base in Locus 89. This sample provided a date much earlier than that of the other samples, presumably because of the “old wood

effect.” The possibility of an “old wood effect” should also be considered in the case of sample RTT-2963 since it consisted of charcoal from a wooden plank inserted into a threshold.

Chronological Ordering of the Samples

The ^{14}C samples can be arranged chronologically on the basis of the stratigraphic information described above (see Table 1). They document a continuous sequence from the Late EB IB to the end(?) of the EB II, and then from the second half or second third of the EB III until the end of the EB III. The current hypothesis is that the latest Early Bronze Age strata at Yarmuth (i.e. strata B-1, G-2, J-1, and K-1) immediately precede the late 3rd millennium abandonment of the site and date indeed from the very end of EB III period since no pottery later than the one found in these strata has been reported from any southern Levantine sites (for details see de Miroschedji 2000:319, 340). Hence, the sequence spanned by the ^{14}C dates incorporates a hiatus corresponding to strata C-5 to C-3 in Area C, i.e. to the first third or first half of the EB III period, a phase labeled “EB IIIA.” The length of this hiatus is impossible to estimate precisely; it could be 1 or 2 centuries.

RADIOCARBON SAMPLES: PREPARATION AND ANALYSIS

The 40 samples of charcoal and short-lived charred materials from Tel Yarmuth were dated at the Weizmann Institute Kimmel Center for Archaeological Sciences in Rehovot, Israel. The acid-base-acid protocol was used to remove contamination as described in Yizhaq et al. (2005). For the small samples like charred seeds, Fourier transform infrared (FTIR) analysis was performed after pretreatment in order to verify the absence of clay in the residual material (Yizhaq et al. 2005). After pretreatment, the ^{14}C concentrations were measured either by liquid scintillation counting (LSC) or by accelerator mass spectrometry (AMS) depending from the size of the sample after pretreatment. The data regarding the sample, context, type, and age are given in Table 2 in stratigraphic order.

Table 2 Results and details of the context of all the samples measured from Tel Yarmuth. The samples are listed in stratigraphic order. Short-lived material samples are marked with an asterisk after the sample number. Note the following abbreviations in the column “Archaeological context”: Sq. = square; Str. = Stratum; L = Locus; B = Basket.

| Lab code | Age | Calibrated $\pm 1 \sigma$ yr BC | Calibrated $\pm 2 \sigma$ yr BC | Archaeological context |
|-----------|---------------|---|--|--|
| RTT-5904* | 4455 \pm 60 | 3331 (32.4%) 3215 3186 (7.4%) 3156 3127 (28.4%) 3023 | 3346 (86.4%) 3006 2990 (9.0%) 2930 | Area C, Sq. Q13; Stratum C-9; L1038-2; field nr TY134; layer above bedrock (same as RTT-5905); seeds |
| RTT-5905* | 4345 \pm 60 | 3078 (2.1%) 3073 3024 (66.1%) 2900 | 3322 (2.4%) 3272 3266 (2.5%) 3236 3171 (0.4%) 3162 3116 (90.1%) 2877 | Area C, Sq. Q13; Stratum C-9; L1038-2; field nr TY141; layer above bedrock (same as RTT-5904); seeds |
| RTA-3499 | 4370 \pm 90 | 3309 (1.2%) 3301 3282 (0.9%) 3277 3265 (4.7%) 3240 3105 (61.5%) 2892 | 3354 (95.1%) 2872 2799 (0.2%) 2794 2783 (0.1%) 2781 | Area C, Sq. P15; Stratum C-9 or C-8; L392-1+2; B9293b; charcoal |
| RTT-5902* | 4420 \pm 60 | 3311 (3.4%) 3295 3285 (2.2%) 3275 3265 (6.9%) 3239 3106 (55.7%) 2923 | 3336 (25.7%) 3210 3193 (6.4%) 3151 3139 (63.3%) 2911 | Area C, Sq. R12; Stratum C-8; base of L1055; field nr TY 118; seeds |
| RTT-5903* | 4330 \pm 55 | 3014 (68.2%) 2897 | 3264 (1.0%) 3246 3101 (94.4%) 2874 | Area C, Sq. R12; Stratum C-8; L1052 (floor at the junction of L1052A and B); field nr TY 119; seeds |
| RTA-3498 | 4385 \pm 55 | 3090 (16.1%) 3047 3033 (52.1%) 2917 | 3327 (11.3%) 3231 3225 (0.5%) 3219 3176 (1.4%) 3160 3121 (82.3%) 2896 | Area C, Sq. Q13; Stratum C-8; L1038-1+floor a; B9281b (just above RTT-5904 and -5905); charcoal |

Table 2 Results and details of the context of all the samples measured from Tel Yarmuth. The samples are listed in stratigraphic order. Short-lived material samples are marked with an asterisk after the sample number. Note the following abbreviations in the column "Archaeological context": Sq. = square; Str. = Stratum; L = Locus; B = Basket. (Continued)

| Lab code | Age | Calibrated $\pm 1 \sigma$ yr BC | Calibrated $\pm 2 \sigma$ yr BC | Archaeological context |
|-----------|---------------|---|---|--|
| RTA-3504 | 4330 \pm 45 | 3011 (22.2%) 2977 2971 (11.0%) 2949 2944 (35.0%) 2898 | 3090 (6.7%) 3051 3031 (88.7%) 2882 | Area C, Sq. N18 Stratum C-8 ; L925; B9403; charcoal |
| RTT-5291* | 4300 \pm 40 | 3007 (9.1%) 2989 2931 (59.1%) 2883 | 3024 (95.4%) 2876 | Area C, Sq. O17; Stratum C-8 ; L922-1; B9363; seeds, <i>Scorpiurus</i> sp. |
| RTA-3503 | 4390 \pm 50 | 3089 (15.8%) 3051 3031 (52.4%) 2920 | 3325 (10.4%) 3234 3173 (1.0%) 3161 3118 (83.9%) 2901 | Area C, Sq. N18; Stratum C-8 ; L910-2; B9389; charcoal |
| RTA-3500 | 4360 \pm 60 | 3084 (6.8%) 3066 3028 (61.4%) 2905 | 3324 (7.4%) 3235 3173 (0.7%) 3161 3117 (87.3%) 2883 | Area C, Sq. N17; Stratum C-8 ; L913; B9214; charcoal |
| RTT-5292* | 4380 \pm 40 | 3079 (4.5%) 3071 3025 (63.7%) 2921 | 3264 (1.6%) 3247 3101 (93.8%) 2902 | Area C, Sq. R13; Stratum C-7 ; L609-surface e; B9222b; seeds, <i>Lolium</i> sp. |
| RTA-3497 | 4325 \pm 50 | 3011 (21.1%) 2977 2971 (11.1%) 2949 2944 (36.1%) 2895 | 3091 (8.2%) 3043 3038 (87.2%) 2879 | Area C, Sq. Q14; Stratum C-7 ; L1030-floor c=L1051; B9279b; charcoal |
| RTA-3496 | 4365 \pm 50 | 3079 (3.7%) 3071 3025 (64.5%) 2911 | 3310 (0.7%) 3297 3284 (0.4%) 3276 3265 (2.4%) 3240 3106 (92.0%) 2889 | Area C, Sq. Q13-14; Stratum C-7 ; L1030-floor a; B9227b; charcoal |
| RTA-3501 | 4425 \pm 55 | 3311 (3.8%) 3295 3286 (2.6%) 3275 3265 (7.5%) 3239 3106 (54.3%) 2927 | 3335 (26.7%) 3211 3192 (6.3%) 3152 3137 (62.4%) 2916 | Area C, Sq. N17; Stratum C-7 ; L657-3+floor c; charcoal |
| RTA-3502 | 4470 \pm 90 | 3339 (32.3%) 3206 3196 (26.2%) 3082 3069 (9.7%) 3026 | 3370 (95.4%) 2910 | Area C, Sq. O17; Stratum C-6A ; L922-1+Tr.931-2; B9383; charcoal |
| RTT-5289* | 4410 \pm 40 | 3095 (43.1%) 3006 2991 (25.1%) 2930 | 3325 (13.1%) 3234 3173 (1.2%) 3161 3118 (81.1%) 2914 | Area Jc, Sq. H42; Phase Jc-3 ; L2821; B17567 (same as RTT-5290); seeds, <i>Lolium</i> sp. |
| RTT-5290* | 4360 \pm 40 | 3016 (68.2%) 2916 | 3091 (95.4%) 2900 | Area Jc, Sq. H42; Phase Jc-3 ; L2821; B17567 (same as RTT-5289); seeds, cereals |
| RTT-5288* | 4340 \pm 40 | 3011 (24.0%) 2978 2971 (13.8%) 2949 2944 (30.4%) 2905 | 3087 (5.6%) 3061 3030 (89.8%) 2890 | Area Jc, Sq. H42; Phase Jc-3 ; L2819-1 (layer of black ashy earth sealed by plastered surface); B17551; seeds, Lens |
| RTA-3493 | 4300 \pm 55 | 3011 (15.9%) 2977 2971 (1.9%) 2966 2961 (4.8%) 2949 2944 (45.6%) 2880 | 3091 (89.7%) 2862 2807 (5.0%) 2758 2718 (0.7%) 2708 | Area Bd, Sq. L39; Stratum Bd-2 (corresponding to Str. J-4); L1805-1; B14039; charcoal |
| RTA-3505 | 4135 \pm 50 | 2870 (19.7%) 2800 2760 (48.5%) 2620 | 2880 (95.4%) 2570 | Area G, Sq. AB33; Stratum G-3 ; L1298-floor a; B12276; charcoal |
| RTA-3506 | 4100 \pm 50 | 2855 (15.7%) 2812 2747 (6.9%) 2725 2697 (45.6%) 2577 | 2873 (90.6%) 2566 2524 (4.8%) 2496 | Area G, Sq. X31; Stratum G-3 ; L1279-1; B12321; charcoal |
| RT-3508 | 4342 \pm 50 | 3013 (68.2%) 2905 | 3096 (95.4%) 2885 | Area G, Sq. X31; Stratum G-3 ; paved threshold between L1234 and L1219; B12510; charcoal |
| RTT-5283* | 4150 \pm 70 | 2873 (12.8%) 2834 2818 (51.2%) 2662 2649 (4.2%) 2635 | 2896 (93.9%) 2569 2516 (1.5%) 2500 | Area Ja, Sq. K41-42; Stratum J-3 ; L2104 (black ashes on floor 2104-a); B17561; seeds |
| RTT-5285* | 4240 \pm 70 | 2919 (29.5%) 2850 2813 (26.6%) 2741 2729 (10.5%) 2694 2687 (1.5%) 2680 | 3021 (95.4%) 2620 | Area Ja, Sq. K44; Stratum J-3 ; L2137-2 + floor b; B17583; seeds |

Table 2 Results and details of the context of all the samples measured from Tel Yarmuth. The samples are listed in stratigraphic order. Short-lived material samples are marked with an asterisk after the sample number. Note the following abbreviations in the column "Archaeological context": Sq. = square; Str. = Stratum; L = Locus; B = Basket. (Continued)

| Lab code | Age | Calibrated $\pm 1 \sigma$ yr BC | Calibrated $\pm 2 \sigma$ yr BC | Archaeological context |
|-----------|-----------------------|---|--|---|
| RTT-5286* | 3795 \pm 40 | 2290 (54.8%) 2195 2172 (13.4%) 2145 | 2434 (0.8%) 2422 2404 (2.1%) 2379 2349 (89.3%) 2130 2087 (3.2%) 2049 | Area Ja, Sq. K41-42; Stratum J-3 ; L2137-1+2 (ashy earth); B17611; seeds, cereals |
| RTT-5295* | 4135 \pm 40 | 2864 (13.4%) 2830 2822 (5.8%) 2807 2759 (16.8%) 2717 2711 (32.2%) 2628 | 2875 (89.7%) 2617 2611 (5.7%) 2581 | Area Ba, Sq. Q26; Stratum B-2 ; L2632; B17159 (beneath RTT 5293 and RT 5294 of L89; same as RTT 5296); seeds, cereals |
| RTT-5296* | 4250 \pm 40 | 2911 (55.1%) 2870 2802 (13.1%) 2778 | 2926 (62.7%) 2849 2814 (25.8%) 2740 2730 (6.4%) 2693 2687 (0.5%) 2679 | Area Ba, Sq. Q26; Stratum B-2 ; L2632; B17151+B17159+B17169 (beneath RTT 5293 of L89; same as RTT 5295); seeds, cereals |
| RT-2969 | 4420 \pm 25 | 3261 (1.7%) 3257 3097 (65.4%) 3012 2948 (1.1%) 2945 | 3310 (1.1%) 3297 3284 (0.7%) 3276 3266 (6.1%) 3240 3106 (87.5%) 2923 | Area Ba, Sq. Q26; Stratum B-1 ; Palace B1, L89-floor a (above RTT 5295 and 5296 from L2632); B13431. Fragment of a wooden post; probable old wood effect; charcoal |
| RT-2966 | 4215 \pm 65 | 2903 (22.7%) 2850 2813 (30.7%) 2742 2729 (12.9%) 2694 2687 (2.0%) 2680 | 2924 (93.2%) 2617 2611 (2.2%) 2581 | Area Ba, Sq. Q28; Stratum B-1 ; Palace B1, L1619; B13333; charcoal |
| RTT-5293* | 4210 \pm 40 | 2892 (23.3%) 2860 2809 (36.4%) 2756 2720 (8.5%) 2704 | 2905 (31.6%) 2835 2816 (63.8%) 2668 | Area Ba, Sq. Q26; Stratum B-1 ; Palace B1, L89- floor a (seeds on floor); B17150 (same as RTT 5294); seeds, cereals |
| RTT-5294* | 4180 \pm 40 | 2880 (14.4%) 2851 2813 (37.3%) 2743 2727 (15.6%) 2695 2683 (0.9%) 2681 | 2891 (22.1%) 2831 2821 (73.3%) 2631 | Area Ba, Sq. Q26; Stratum B-1 ; Palace B1, L89 (seeds on floor); B17168 (same as RTT 5293); seeds, cereals |
| RT-2963 | 4115 \pm 35 | 2860 (20.3%) 2810 2750 (9.4%) 2720 2700 (38.5%) 2580 | 2880 (24.5%) 2800 2780 (70.9%) 2570 | Area Bb, Sq. T37; Stratum B-1 ; Palace B1, L2018 floor; B15053 or B15059? Charcoal from plank on threshold: possible old wood effect; charcoal |
| RT-2964 | 4105 \pm 50 | 2860 (16.3%) 2810 2750 (7.4%) 2720 2700 (44.5%) 2570 | 2880 (91.4%) 2560 2530 (4.0%) 2490 | Area Bb, Sq. S 38; Stratum B-1 ; Palace B1, L2025 floor; B15112; charcoal |
| RT-3495 | 4100 \pm 23 | 2840 (14.4%) 2810 2670 (53.8%) 2570 | 2860 (22.0%) 2800 2750 (6.9%) 2720 2700 (66.5%) 2570 | Area Bb, Sq. T40; Stratum B-1 ; Palace B1, L1970; B15666. Sample taken from layer of debris on the floor; charcoal |
| RT-2967 | 4035 \pm 95 | 2853 (7.9%) 2813 2745 (3.1%) 2726 2696 (57.1%) 2466 | 2878 (94.6%) 2339 2322 (0.8%) 2309 | Area Bb, Sq. S36-37; Stratum B-1 ; Palace B1, L2012-1; B15174; charcoal |
| RT-2968 | 3980 \pm 40 | 2569 (40.4%) 2517 2500 (27.8%) 2467 | 2618 (0.7%) 2610 2581 (90.3%) 2400 2382 (4.4%) 2347 | Area Ba, Sq. R 25; Palace B1, Stratum B-1 ; L80-1 to 3 + floor a; B13071; charcoal |
| RT-2965 | 3565 \pm 40 | 2009 (2.3%) 2002 1977 (62.5%) 1879 1839 (3.4%) 1830 | 2026 (76.5%) 1865 1849 (18.9%) 1773 | Area Ba, Sq. R29; Stratum B-1 ; Palace B1, L1647-1+floor a; B13341; Palace B1; charcoal |
| RTA-3507 | 45,150 \pm 550 | | | Area G, Stratum G-2 ; L1418-floor c; B12490; charcoal |
| RTT-5284* | 131.3 \pm 05 pMC | modern | | Area Ja; Stratum J-3 ; L2104; B17575; Thymelaeaceae |
| RTT-5287* | 110.0 \pm 03 pMC | modern | | Area Ja; Stratum J-3 ; L 2819; B17550; <i>Pisum</i> |

^{14}C ages are reported in conventional ^{14}C yr BP (AD 1950) in accordance with international convention (Stuiver and Polach 1977). Thus, all calculated ^{14}C ages have been corrected for fractionation as to refer the results to be equivalent with the standard $\delta^{13}\text{C}$ value of -25‰ . All the samples have $\delta^{13}\text{C}$ values between -22‰ and -27‰ . The only exception is sample RTT-3507 ($\delta^{13}\text{C} = -29.0\text{‰}$). All ^{14}C ages were calibrated using OxCal v 4.1.6 (Bronk Ramsey 2009a) and the IntCal09 data (Reimer et al. 2009) calibration curve. Analysis and modeling of the dates based on archaeological information was performed using the Bayesian method and the mathematical tools as given in OxCal v 4.1.6.

Two of the samples, RTT-5284 and RTT-5287, both originating from Subarea Ja, were found to be modern (intrusive), and 1 sample, RTA-3507, provided an age of $45,150 \pm 550$ yr uncalibrated. This sample was probably a piece of asphalt used in antiquity (Aufderheide et al. 2004). After removal of these 3 samples, 37 dates were used for building a chronology for Tel Yarmuth: 3 samples (2 seeds, 1 charcoal) originate from “Late EB IB” contexts, 15 samples (7 seeds, 8 charcoals) from EB II contexts, 7 samples (3 seeds, 4 charcoals) from EB IIIB contexts, and 12 samples (4 seeds, 8 charcoals) from EB IIIC contexts (Table 2).

MODELING

Various Bayesian models were applied in order to determine the most reliable dates of transition between the archaeological layers. Four types of models were applied: Simple model, Detailed model, a model with an imposed gap, and a model with gap with *terminus post quem* (henceforth TPQ) of 2900 ± 10 yr BC for the beginning of the gap. Each of these models was again separated into models of seeds only and charcoal only in order to evaluate the possible old-wood effect. Outliers identified after the modeling were excluded and the model was run without the outliers. In case an end of a previous phase is given by a short-lived sample that is an outlier, while the beginning of the following phase is given by charcoal sample, we preferred to remove the charcoal because of the possibility of the old-wood effect.

As a general rule, any single date that had an agreement of less than 60% was considered an outlier. However, some samples close to the 60% cut-off will be just above or below the 60% cut-off when a model is run a few times. If more than 1 sample was identified as an outlier, the removal was done stepwise, namely the one with the lowest agreement was removed first. The model was run again after removal of each outlier, to verify if the removal of the sample(s) would cause a change in the agreement of the rest of the samples.

The models are built using phases or sequences, following the archaeological information. If a model was built using phases, the samples within each phase were ordered from oldest to youngest. This does not indicate that the samples were necessarily found in that order in the archaeological layers. If the model was built using sequences, the samples are ordered according to archaeological stratigraphic order. OxCal v 4.1.6 (Bronk Ramsey 2009a) software was used to calculate the transitions.

Structure of the Models

Simple models: The data were separated according to their association to Final EB I, EB II, or EB III cultural materials. In the Simple model, the dates were ordered as phases, since it was not possible to know the exact stratigraphic order of the samples within each period. Inside the phases, dates were ordered from old to young independent of the stratigraphy. The Final EB I to EB II transition is “contiguous,” implying that as the previous period ended, the following started (see OxCal v 4.1). The EB II to EB IIIB transition is “sequential” due to the gap in the ^{14}C data. This model should pro-

vide the transition between the Final EB I and EB II and the end range for EB II and beginning range for EB IIIB.

Detailed models: In this model, the data are separated according to the detailed stratigraphic sequence of the site. Several samples from layers C-8, C-7, C-6A, and Jc-3 had additional information about their inner ordering within the layer indicating which samples were found one above the other. Accordingly, for these layers the samples were ordered as sequences, while the samples that had no additional indication of their relative placement in the strata were placed in the sequence according to their ^{14}C age. Where no information on the relative placement was available, the samples were ordered in phases, also from oldest to youngest, even though this does not affect the modeling. The transitions between phases or sequences are contiguous, except in the case of the EB II-EB IIIB boundary, where it is sequential due to the absence of datable ^{14}C samples from strata C-5, C-4, C-3, covering the EB IIIA period.

Models with a gap: The length of the EB IIIA period at Tel Yarmuth lacking ^{14}C dates was estimated to be between 100 to 200 yr. Therefore, separate models were run by inserting a gap of 150 ± 50 yr between the EB II and EB IIIB layers. These models have the same structure as the Simple and the Detailed models described above.

Models with a gap and a *terminus post quem* (TPQ): A *terminus post quem* was inserted before the 150 ± 50 yr gap. This was done in order to determine whether it would be possible to stabilize the end of the EB II period around 2900 BC.

RESULTS

In Figures 3, 4, 6, and 7, all the models are shown with all the dates, including the outliers. Outliers are identified by the code [P] and a question mark after the sample number and they are plotted in dark gray only (e.g. samples RTT-5291 and RT-2969 in Figure 3). Even though they are seen in the plot, they do not affect the model. The general agreement of the model is given on top of the multiplot, written as [Amodel:xxx] (e.g. in the Simple model Figure 3 the general agreement is 123). After each ^{14}C date, the sample number appears first, and nearby is given the amount of agreement [A:xxx] of each individual date within the model (e.g. in Figure 3 sample RTT-5904 has an A value of 95). The light gray single plots describe the whole span of possible dates as determined by the calibration combined with laboratory error. The probability distributions marked with dark gray define the modeled results.

EB I-II and EB II-III Transitions According to the Simple and Detailed Models

The Simple model has 2 outliers (RTT-5291, RT-2969). The agreement of the model was 94 before their removal and 123 after (Table 3). As a result, the EB II end and EB IIIB begin dates were lowered by about 30 yr. According to the Simple model, the EB I-II transition took place between 3030–2970 BC and the EB II ended by 3000–2930 BC (Figure 3). The EB IIIB began between 2960–2910 BC. These dates are significantly higher than the conventionally accepted dates (see above). If only seed samples are used, the EB I-II lower limit of the transition becomes younger by 20 yr. The EB II ends between 2980–2910 BC, and EB IIIB starts between 2950–2850 BC, up to 60 yr later than when charcoal samples are also used.

In the Detailed model, the major transitions turn out to be very similar to the Simple model, but they are more spread by few decades (Figure 4, Table 3). The EB I-II transition range is 3050–2980 BC, being up to 20 yr older than in the Simple model. The EB II ends 2960–2910 BC, which is a date up to 40 yr younger than in the Simple model. The EB IIIB begins also ~30 yr later (2930–2880 BC).

Table 3 Modeled ranges for EB I-II transition, EB II end, and EB IIIB begin ranges in all the models. The transition limit is given in relation to the $\pm 1 \sigma$.

| Name of the model | EB I-II | EB II end | EB IIIB begin | Dates | Outliers removed | Agreement |
|---|-----------|-----------|---------------|-------|---|-----------|
| Simple with outliers | 3030–2990 | 3010–2960 | 2990–2940 | 37 | — | 94 |
| Simple | 3030–2970 | 3000–2930 | 2960–2910 | 35 | 5291, 2969 | 123 |
| Simple seeds | 3030–2950 | 2980–2910 | 2950–2850 | 16 | 5291 | 90 |
| Simple charcoal | 3040–2970 | 3010–2940 | 2970–2910 | 21 | 2969 | 119 |
| Simple with gap 150 \pm 50 yr | 3030–2980 | 3010–2950 | 2840–2770 | 33 | 5291, 2969, 3508, 3493, 5296 | 110 |
| Simple seeds with gap | 3040–2970 | 3010–2940 | 2830–2750 | 14 | 5291, 5296 | 83 |
| Simple charcoal with gap | 3040–2960 | 3000–2920 | 2820–2720 | 18 | 2969, 3508, 3493 | 112 |
| Simple with gap 150 \pm 50 yr | 3010–2930 | 2920–2890 | 2770–2720 | 33 | 2969, 3508, 3493, 5285 | 87 |
| TPQ 2900 \pm 10 BC | | | | | | |
| Simple seeds with gap 150 \pm 50 yr | 3020–2930 | 2920–2880 | 2760–2700 | 14 | 5296, 5293 | 74 |
| TPQ 2900 \pm 10 BC | | | | | | |
| Simple charcoal with gap 150 \pm 50 yr | 3050–2940 | 2920–2880 | 2760–2700 | 18 | 2969, 3508, 3493 | 104 |
| TPQ 2900 \pm 10 BC | | | | | | |
| Detailed | 3050–2980 | 2960–2910 | 2930–2880 | 32 | 5291, 3508, 5286, 5296, 2969 | 122 |
| Detailed seeds | 3040–2950 | 2950–2890 | 2920–2860 | 14 | 5286, 5296 | 125 |
| Detailed charcoal | 3060–2980 | 2970–2910 | 2940–2880 | 19 | 3508, 2969 | 110 |
| Detailed with gap 150 \pm 50 yr | 3050–2980 | 2970–2910 | 2810–2740 | 30 | 5291, 3508, 5286, 5296, 2969, 3493, 5293 | 106 |
| Detailed with gap 150 \pm 50 yr | 3050–2980 | 2920–2880 | 2760–2710 | 28 | 5291, 3508, 5286, 5296, 2969, 3493, 5293, 2966, 5294 | 125 |
| TPQ 2900 \pm 10 BC | | | | | | |

Since the Detailed model comprises 8 separate phases, it is very efficient in pinpointing outliers. Out of the 37 samples, 5 are below 60% agreement, and were accordingly removed from the final model. The samples RTT-5286 and -2969 are clear outliers, and cannot be placed in the model in the given stratigraphic position. As pointed out by the excavator (see above), the sample RT-2969 has very probably a significant old-wood effect since it is a fragment of charcoal from a wooden post resting on a stone base. The seed sample RTT-5286 from Stratum Ja-3 is probably intrusive. It should be noted that out of the 5 samples dated from this area, 2 were found modern, indicating some clear disturbance in this vicinity. The seed sample RTT-5291 found under City Wall A in Area C is somewhat surprisingly young. Sample RT-3508 from Stratum G-3 is likely affected by an old-wood effect, and sample RTT-5296 from Stratum B-2 is not a striking outlier, although it may be an intrusion from the overlying layer.

The “Final EB I”-II transition in all 6 Simple and Detailed models (Simple, Simple seeds only, Simple charcoal only, Detailed, Detailed seeds only, and Detailed charcoal only) is more or less the same: it starts between 3060–3030 BC and ends between 2980–2950 BC (see Figure 5, black bars, and Table 4). The 30-yr variability in ranges is probably due to a minor old-wood effect since it corresponds to the differences between the “seeds only” and the “charcoal only” models. In the same 6 models, the “EB II end” ranges have slightly greater variance, from 3010–2950 to 2940–2890 BC (Figure 5, white bars). In this transition as well, the “charcoal only” results are older by 20–60 yr. Similar discrepancies between short-lived material and samples with a possible old-wood effect are apparent in the dates for the beginning of EB IIIB: 2970–2920 BC and 2910–2850 BC (Figure 5, gray bars).

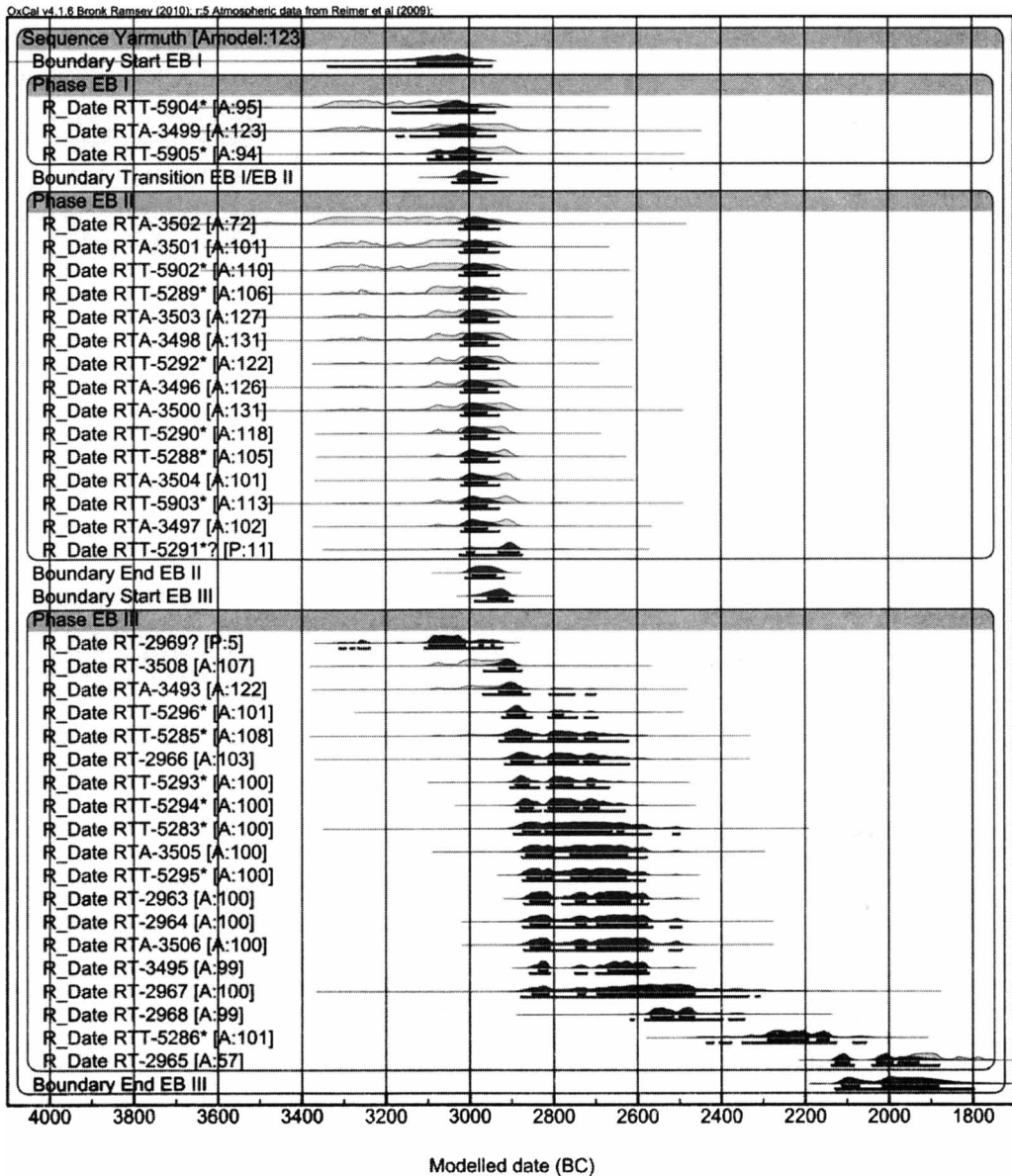


Figure 3 The Simple model: Simple “Final EB I,” EB II, EB III transitions, using seeds and charcoal samples together. Two outliers are marked with a “P” and excluded from the analysis.

Even when the latest date of 2890 BC for the end of EB II is taken as the actual end of the period, the dates remain older than currently accepted by ~200 yr. Furthermore, the beginning of EB IIIB starts before 2850 BC, leaving a short duration of 40 yr for the EB IIIA period (instead of the 100–200 yr accepted conventionally). If a longer EB IIIA period is more likely, the EB II period could have ended as early as 3010 BC based on our results, leaving 160 yr of duration for the EB IIIA period. It is important to stress that in any combination these dates are older than expected, and allow a short duration for the EB IIIA period. For this reason, it was decided to test the insertion of a gap of 150 ± 50 yr to the model between the end of EB II and the beginning of EB IIIB.

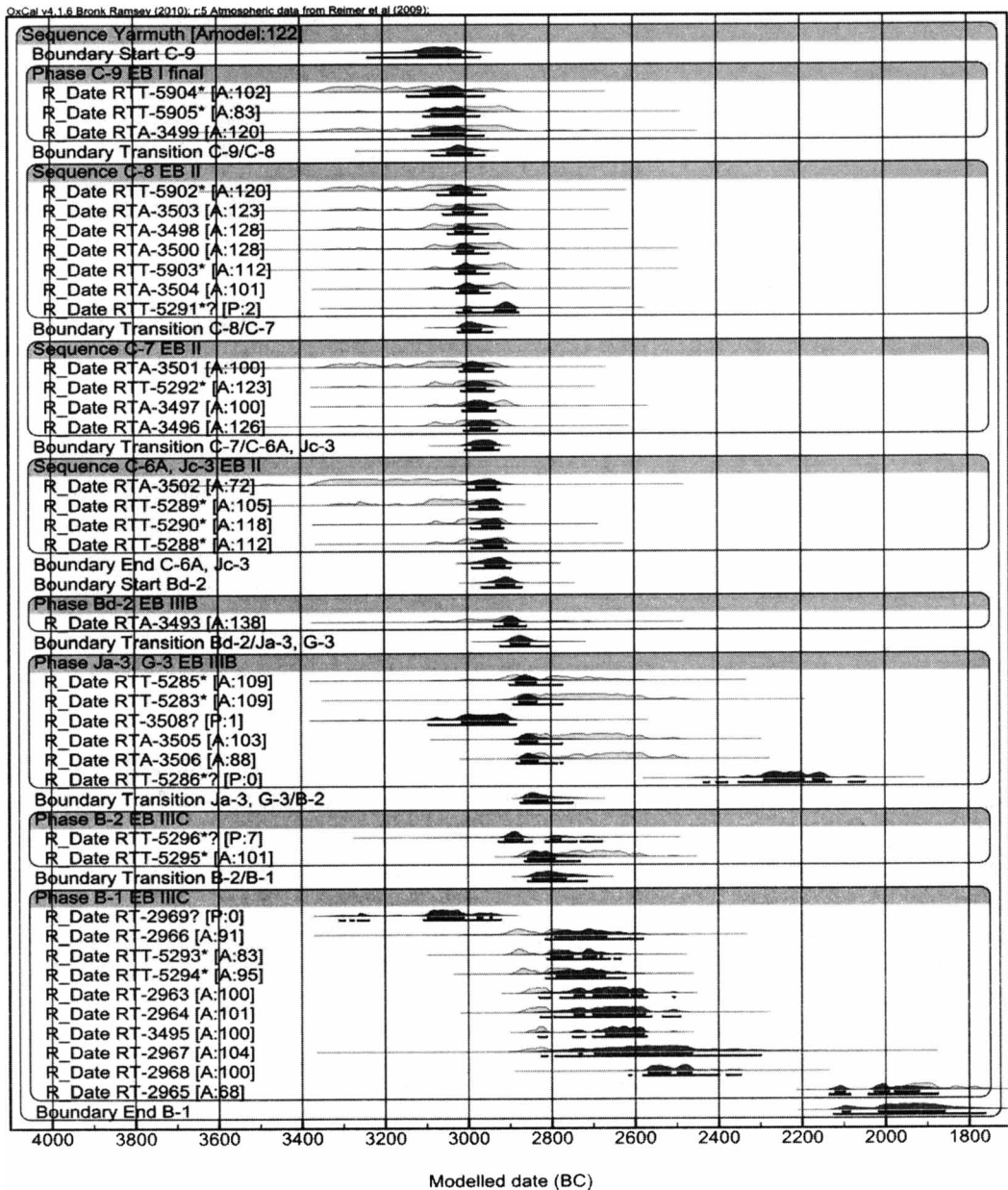


Figure 4 The “Detailed” model

Models with Inserted Gap and TPQ

The insertion of the 150 ± 50 yr gap after the end of the EB II period in the Simple model shifted the end of that period upward by only 10–20 yr (3010–2950 BC) compared to the original Simple model (3000–2930 BC). In contrast, the beginning of the EB IIIB period was shifted downward by as much as 120–140 yr, to 2840–2770 BC (Figure 5 and Table 4). This model has 5 outliers (compared to 2 outliers in the Simple model), from which 4 out of the 5 appear as outliers also in the Detailed model

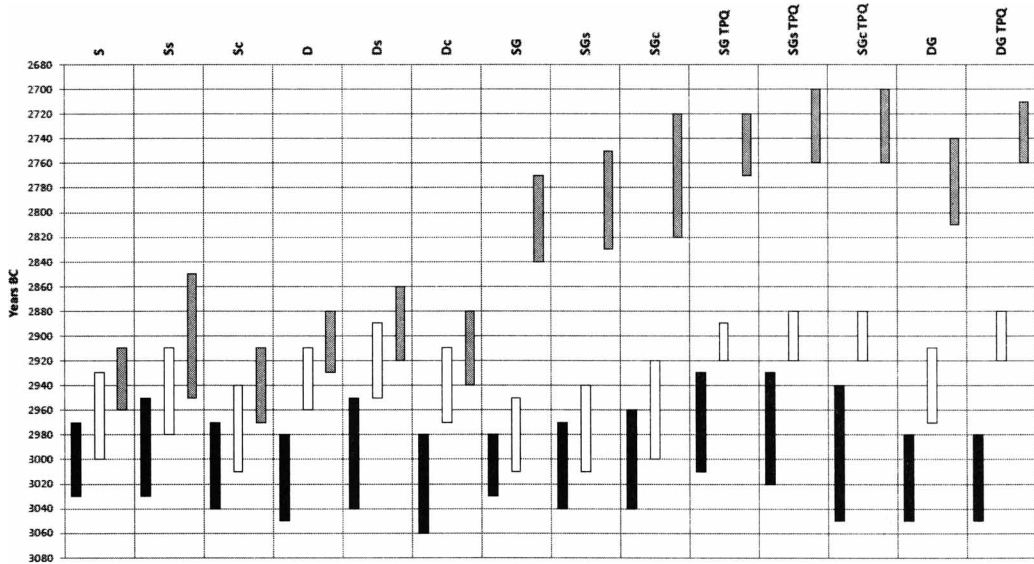


Figure 5 A summary of transition dates according to the various models. S: Simple model. s: Seeds samples only. c: Charcoal samples only. D: Detailed model. G: Gap included. TPQ: Terminus post quem. Black bars: EB I-II transition. White bars: End of EB II. Grey bars: Beginning of EB III B.

without the gap. Interestingly, the “Simple model of charcoal only with gap” yielded younger transitions than the “Simple model of seeds only with gap” model. This further supports that the old-wood effect at Tel Yarmuth is a minor one in general. When the same gap of 150 ± 50 yr was inserted in the Detailed model, the beginning of EB III B moved further downward to 2810–2740 BC, but retained nevertheless the 120–140 yr difference from its original model (Figure 6). Also in this case, the number of outliers increases from 5 to 7 outliers in the “Detailed model with gap.”

The insertion of the 150 ± 50 yr gap into the various models resulted in a slight shortening of the EB II period, which is difficult to reconcile with current historical and archaeological reconstructions that ascribe for this period a much longer duration. In order to prevent an excessive shortening, it was decided to place a constraint for the end of the EB II period. Since the end of the EB II did not occur later than 2900 ± 10 BC in both the Simple and the Detailed models, it was decided to select this date as the most suitable *terminus post quem* (TPQ). As a result, in the Simple models with gap and TPQ, all periods shifted downwards by 20–70 yr. The beginning of the EB III B period shifts accordingly to 2770–2720 BC in both the Simple and the Detailed models, irrespective of the type of sample, seeds or charcoal. Interestingly, the number of outliers in the Simple model with gap and TPQ is lower than in the Simple model with gap without TPQ (4 outliers instead of 5). On the other hand, in the Detailed model with gap and TPQ (Figure 7), 9 samples turn out to be outliers, compared to 7 outliers in the Detailed model with gap without TPQ.

Transitions between Individual Archaeological Strata at Site According to Detailed Models

When the Detailed models with seeds only or with charcoal only are run, the results for the boundaries are very similar. This implies that the old-wood effect is very small, if any. It is important to note that the sequence of archaeological phases in the 2 models is different. In the sequence of charcoal only, the Stratum B-2 is absent, while in the sequence of seeds only, the Stratum Bd-2 is absent (see Table 4). Therefore given the similarity of the boundaries between the 2 models, even with

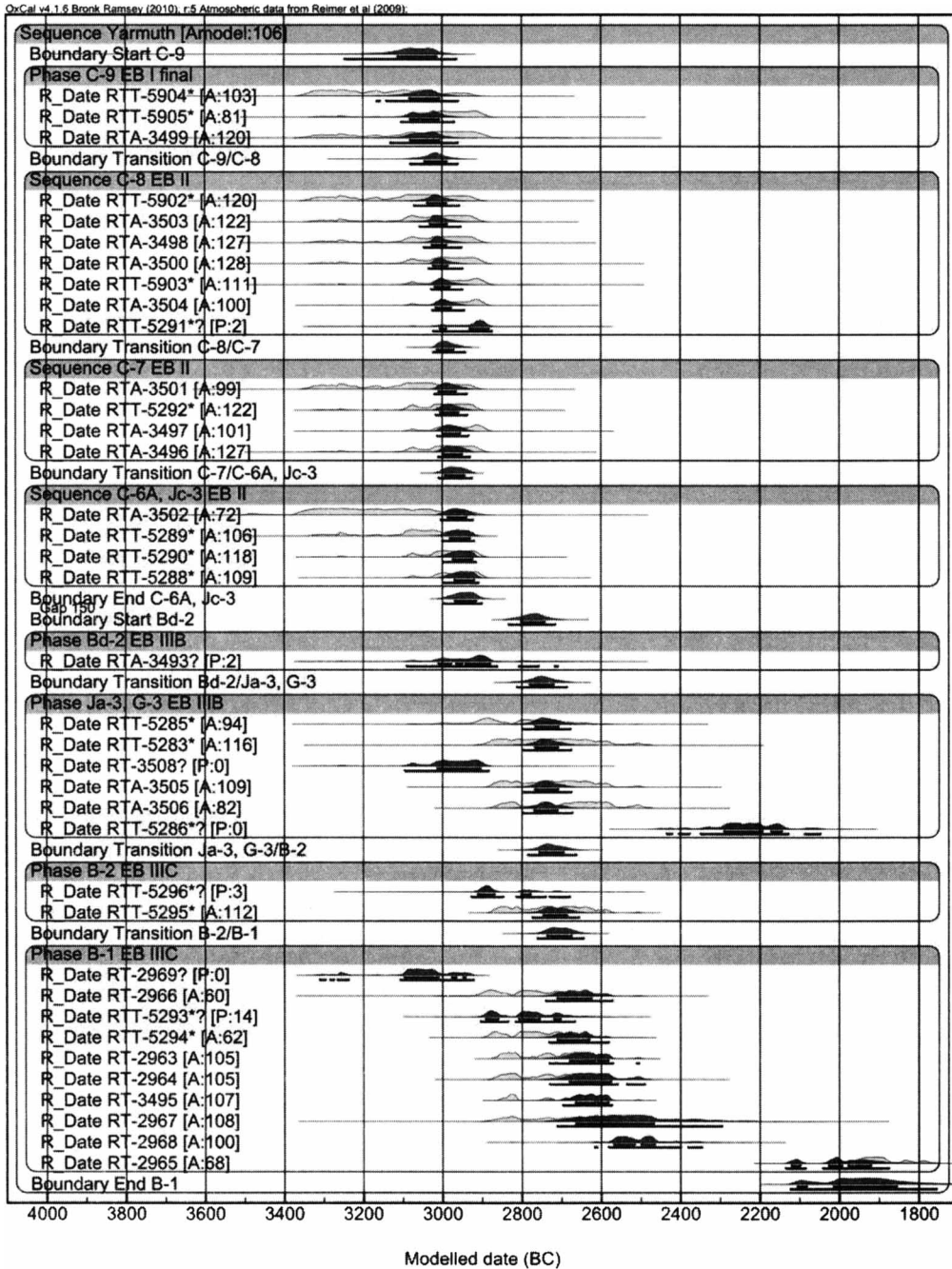


Figure 6 Detailed model with inserted gap of 150 ± 50 yr

some differences in the strata, it was decided to build the final model using all the samples together, covering more phases. The models with gap and gap with TPQ were built using the same set of data. The ranges of the transitions as they appear in the various models are summarized in Table 4.

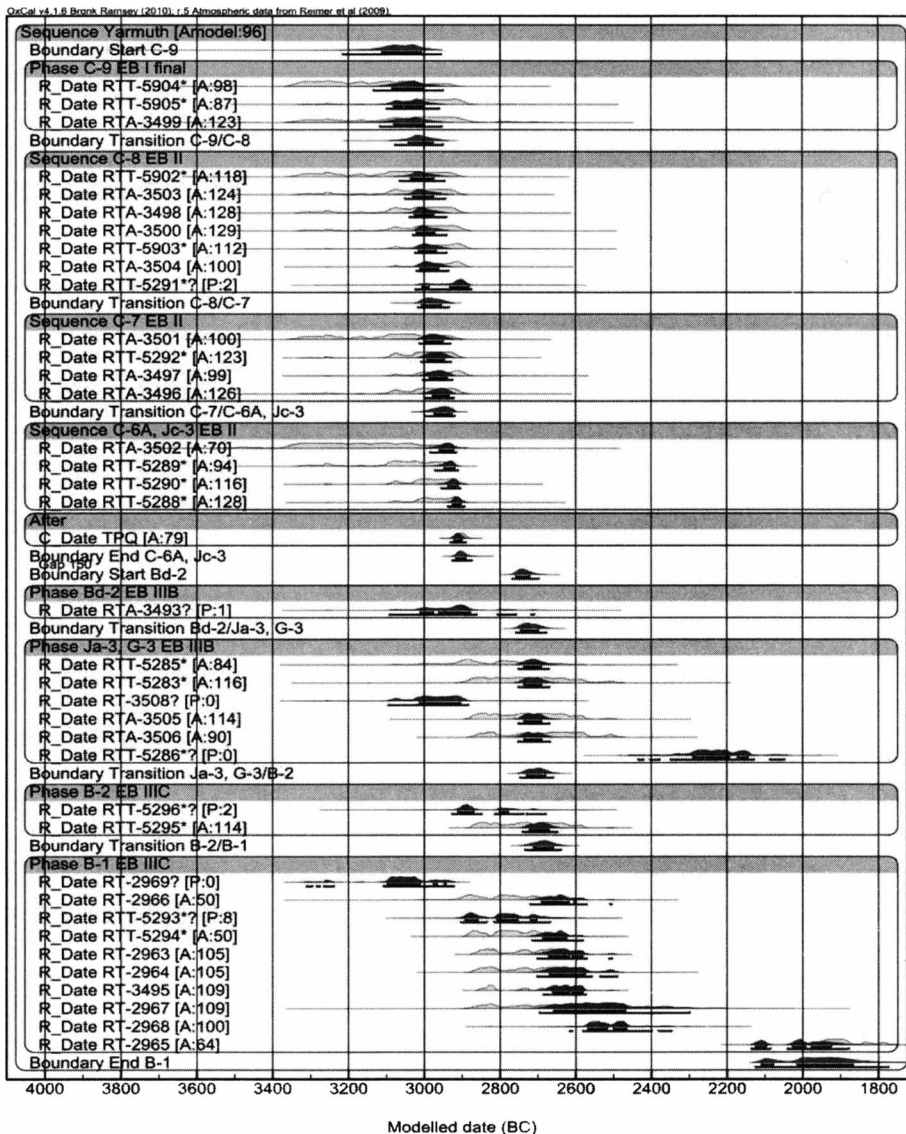


Figure 7 Detailed model with a gap of 150 ± 50 yr and a *terminus post quem* of 2900 ± 10 BC

DISCUSSION

The 37 dates of Tel Yarmuth provide a good framework for the chronology of the Final EB I, the EB II, and the EB III periods in Israel. The Bayesian modeling applied to the Tel Yarmuth data set using the different approaches as explained above, identified from a minimum of 2 to a maximum of 9 outliers. By increasing the level of detail and constrains in the model, the number of outliers grows. The data indicate that at Tel Yarmuth the old-wood effect is not very significant, being between 20–60 yr in Simple models and ~ 20 yr in the Detailed models. The actual effect is probably due to a few specific samples that are clearly defined as outliers (especially RT-2969, RT-3508).

Table 4 Transition dates according to the different Detailed models.

| Boundary (phase) | Seeds and charcoal, 37 samples (5) A = 122 | | Seeds only, 16 samples (3) A = 125 | | Charcoal only, 21 samples (2) A = 110 | | Seeds and charcoal with 150 ± 50 gap, 37 samples (7) A = 106 | | Seeds and charcoal with a gap of 150 ± 50 TPQ, 37 samples (9), A = 125 | |
|--------------------------------|--|-----------|--|-----------|---|-----------|---|-----------|--|-----------|
| | ±1 σ | ±2 σ | ±1 σ | ±2 σ | ±1 σ | ±2 σ | ±1 σ | ±2 σ | ±1 σ | ±2 σ |
| EB I final-EBIIe C-9/C-8 | 3120-3010 | 3240-2960 | 3040-2950 | 3080-2930 | 3060-2980 | 3110-2950 | 3050-2980 | 3090-2960 | 3050-2980 | 3080-2950 |
| EBIIe/IIIm C-8/C-7 | 3020-2960 | 3030-2930 | 3010-2940 | 3040-2920 | 3020-2960 | 3080-2920 | 3020-2970 | 3030-2940 | 3010-2960 | 3020-2930 |
| EB IIIm/II L C-7/C-6A, Ic-3 | 2990-2930 | 3010-2920 | 2980-2920 | 3010-2910 | 3000-2930 | 3020-2910 | 3000-2940 | 3010-2920 | 2980-2930 | 3000-2920 |
| EB IIL end C-6A, Ic-3 | 2960-2910 | 2990-2890 | 2950-2890 | 2990-2870 | 2970-2910 | 3000-2880 | 2970-2910 | 3000-2900 | 2920-2880 | 2930-2860 |
| EB IIIB start Bd-2 start | 2930-2880 | 2970-2870 | No Bd | No Bd | 2940-2880 | 2980-2780 | 2810-2740 | 2840-2710 | 2760-2710 | 2770-2680 |
| EB IIIB/EB IIIB Bd-2/Ia-3, G-3 | 2900-2850 | 2930-2800 | 2920-2860 | 2940-2790 | 2900-2770 | 2920-2690 | 2780-2720 | 2820-2680 | 2740-2680 | 2760-2650 |
| EB IIIB/EB IIIC Ja-3, G-3/B-2 | 2870-2800 | 2880-2740 | 2890-2810 | 2900-2740 | No B-2 | No B-2 | 2760-2690 | 2790-2660 | 2720-2650 | 2740-2630 |
| EB IIIC/EB IIIC B-2/B-1 | 2850-2760 | 2860-2710 | 2880-2760 | 2880-2710 | 2810-2690 | 2850-2650 | 2740-2670 | 2770-2640 | 2690-2630 | 2720-2600 |

Based on all the different modeling performed, the models that best represent the archaeological stratigraphy and ^{14}C dates are

1. Detailed model (seeds and charcoal samples combined);
2. Detailed model with gap;
3. Detailed model with gap and TPQ.

The Detailed model, divided into 8 separate sequential layers, is built following the stratigraphy, and the boundaries are determined only by the ^{14}C dates. This model has the largest amount of data (32 samples) and a total of 5 outliers. In this model, the boundary between “Final EB I” and EB II falls around 3000 BC. The expected gap in the ^{14}C data (EB IIIA strata) is accounted for by the use of a sequential boundary between EB II and EB IIIB and the time range between the 2 boundaries is at most 170 yr (maximum length individually for EB II is 140 yr and for EB IIIA 80 yr; see Table 4), and most probably around 50–60 yr (EB II ends roughly 2930 BC and EB IIIB begins before 2880 BC). This is a completely different scenario for the EB II, which is traditionally given duration of about 300–400 yr, as well as the EB IIIA, allocated traditionally as 100–200 yr (e.g. de Miroschedji 2000:340).

Relying on historical and archaeological considerations, the 50-yr duration for EB IIIA is considered too short. The addition of a gap of 150 ± 50 yr in the Detailed model increased the EB IIIA duration to a maximum duration of 230 yr. But 2 more samples were turned into outliers (RTT-3493 charcoal, RTT-5293 short-lived), and the beginning of EB IIIB moved to between 2810–2740 BC.

In the Detailed model with gap, the end of EB II remains high and an attempt was made to stabilize it around 2900 BC by inserting a TPQ for the beginning of EB IIIA. This created 2 additional outliers (total 9 outliers), but lowered the beginning of EB IIIB to 2760–2710 BC. These boundaries are closer to the conventional dates, and they leave a reasonably long duration for the EB IIIA and EB II. This identification of 2 more samples as outliers, with no contextual or archaeological explanation raises the question about the other contexts used in the model. Based on the comparison of the various models, and the raw ^{14}C data in this study, it is not straightforward to select the Detailed with gap and TPQ model instead of the Detailed model.

Among the 15 ^{14}C measurements (charcoal and seeds) made on samples from the EB II at Tel Yarmuth, none has a calibrated 1σ range later than 2870 BC. On the other hand, the EB IIIB dates mostly do not start before 2900 BC (except 3 charcoal samples RT-2969, RT-3508, RTA-3493). Thus, the end of the EB II at Tel Yarmuth can be quite confidently established around 2900 BC, some 200 yr earlier than conventionally thought. It is important to note that the end of EB II seems to have taken place precisely when a deep slope exists in the calibration curve, occurring between 2910–2890 BC (corresponding to 4350–4200 uncalibrated). The fact that the measurements are neatly divided on the opposite sides of this slope further adds to the reliability of the date of the transition. The “EB IIIB begin” date can be slightly more flexible, but seems to have taken place in the course of the 29th century, or even during the 28th century. The latter date would imply that some of the ^{14}C samples are either not *in situ* or residual (RTT--5293, -5294) or there is a substantial old-wood effect (RTA-3493, RT-2966).

The end of the EB III in Tel Yarmuth is documented by a series of dates associated with the latest known pottery assemblage of EB IIIC as represented in Palace B1. The samples were gathered on plastered floors and are understood to form a uniform group of dates close to the time of abandonment of the site. All of the dates of this phase end before 2470 BC (except sample RT-2965 that is clearly intrusive). Actually most of the date ranges end before 2580 BC, and if the dates are really

to be seen as an homogeneous group, the sample RT-2968 could be interpreted as secondary use of the ruins after the abandonment Tel Yarmuth. In this case, the end of EB IIIC could be even much earlier.

A lesson learnt from this study is that secure archaeological context is crucial for the accuracy of the model and reliability of the results. Detailed stratigraphy enables effectively to find out the archaeological outliers, like RTT-5286, which appears as an outlier only in the Detailed model. A case like this might bring attention to the context as open to intrusive samples.

The new chronological framework for the “Final EBI”- EB II, and EB III in Tel Yarmuth, taking in consideration the Detailed model and Detailed model with gap and TPQ, can be presented as below:

| Transition “Final EB IB” to EB II: 3050 to 2980 BC | |
|---|--|
| End of EB II (= transition EB II-EB IIIA): 2950–2900 BC, most probably around 2900 BC | |
| Scenario 1 | Scenario 2 |
| Very short EB IIIA (max 70 yr) | EBIIIA of 150 yr duration |
| Beginning of EB IIIB: 2930–2880 BC | Beginning of EB IIIB: 2760–2710 BC |
| End of EB IIIC: before mid-25th century BC | End of EB IIIC: before mid-25th century BC |

CONCLUSION

Based on the modeling of the 37 ¹⁴C dates from Tel Yarmuth, spanning the Early Bronze Age I, II, and III, a new chronology for this period has been proposed. The EB II has been shortened and its end is raised to about 2950–2900 BC. The EB III ends at the latest around 2450 BC, although according to the models an earlier date could be supported. The new ¹⁴C-based chronology of Tel Yarmuth, covering a major part of the EB period, represents a backbone for the EBA chronology in southern Levant.

REFERENCES

- Aufderheide AC, Nissenbaum A, Cartmell L. 2004. Radiocarbon date recovery from bitumen-containing Egyptian embalming resins. *Journal of the Society for the Study of Egyptian Antiquities* 31:87–96.
- Ben-Tor A. 1975. The first season of excavations at Tell Yarmuth: August 1970. *Qedem (Monographs of the Institute of Archaeology, the Hebrew University of Jerusalem)* 1:55–87.
- Ben-Tor A. 1991. New light on the relations between Egypt and southern Palestine during the Early Bronze Age. *Bulletin of the American Schools of Oriental Research* 281:3–10.
- Ben-Tor A. 1992. The Early Bronze Age. In: Ben-Tor A, editor. *The Archaeology of Ancient Israel*. New Haven: Yale University Press. p 81–125.
- Bronk Ramsey C. 2009a. Bayesian analysis of radiocarbon dates. *Radiocarbon* 51(1):337–60.
- Bronk Ramsey C. 2009b. Dealing with outliers and offsets in radiocarbon dating. *Radiocarbon* 51(3):1023–45.
- Bronk Ramsey C, Dee MW, Rowland JM, Higham TFG, Harris SA, Brock F, Quiles A, Wild EM, Marcus ES, Shortland AJ. 2010. Radiocarbon-based chronology for Dynastic Egypt. *Science* 328(5985):1554–7.
- de Miroschedji P. 1999. Yarmuth, the dawn of city-states in southern Canaan. *Near Eastern Archaeology* 62(1): 2–19.
- de Miroschedji P. 2000. An EB III pottery sequence for southern Israel. In: Philip G, Baird D, editors. *Ceramics and Change in the Early Bronze Age of the Southern Levant*. Sheffield: Sheffield Academic Press. p 315–45.
- de Miroschedji P. 2003. The Late EB III Palace B1 at Tel Yarmuth: a descriptive summary. *Eretz Israel* 27:153–70.
- de Miroschedji P. 2008. Jarmuth Tel. In: Stern E, editor. *The New Encyclopedia of Archaeological Excavations in the Holy Land, Volume 5, Supplementary Volume*. Jerusalem: Israel Exploration Society. p 1792–7.
- de Miroschedji P. In press a. Early Bronze Age (Israel, Palestinian territories). In: Killebrew A, Steiner M, editors. *Oxford Handbook of Archaeology of the Levant (ca. 8000–332 BCE)*. Oxford: Oxford University Press.

- de Miroschedji P. In press b. Egypt and southern Canaan in the Third Millennium BCE: Uni's Asiatic campaigns revisited. In: Lehmann G, Gruber MI, Ahituv S, Talshir Z, editors. *All the Wisdom of the East. Studies in Near Eastern Archaeology and History in Honor of Eliezer D. Oren*. Orbis biblicus et orientalis XXX. Fribourg: Fribourg Academic Press.
- de Miroschedji P, Davis S, Goldberg P, Kermorvant A, Nodet E, Rosen S, London G. 1988. *Yarmouth I, rapport sur les trois premières campagnes de fouilles à Tel Yarmouth (Israël), 1980–1982*. Paris: Editions Recherche sur les civilisations.
- Hennessy JB. 1967. *The Foreign Relations of Palestine during the Early Bronze Age*. Colt Archaeological Institute Publication. London: B. Quaritch.
- Hornung E, Kraus R, Warburton DA. 2006. *Ancient Egyptian Chronology*. Leiden: Brill.
- Jimenez Serrano A. 2007. *Los Primeros Reyes y la Unificación de Egipto*. Jaén: Universidad de Jaén.
- Kitchen KA. 1991. The chronology of ancient Egypt. *World Archaeology* 23(2):201–8.
- Mazar A. 1990. *Archaeology of the Land of the Bible 10,000–586 B.C.E.* New York: Doubleday.
- Regev J, de Miroschedji P, Greenberg R, Braun E, Greenhut Z, Boaretto E. 2012. Chronology of the Early Bronze Age in the southern Levant: new analysis for a High Chronology. *Radiocarbon*, these proceedings.
- Reimer PJ, Baillie MGL, Bard E, Bayliss A, Beck JW, Blackwell PG, Bronk Ramsey C, Buck CE, Burr GS, Edwards RL, Friedrich M, Grootes PM, Guilderson TP, Hajdas I, Heaton TJ, Hogg AG, Hughen KA, Kaiser KF, Kromer B, McCormac FG, Manning SW, Reimer RW, Richards DA, Southon JR, Talamo S, Turney CSM, van der Plicht J, Weyhenmeyer CE. 2009. IntCal09 and Marine09 radiocarbon age calibration curves, 0–50,000 years cal BP. *Radiocarbon* 51(4): 1111–50.
- Shaw I, editor. 2000. *The Oxford History of Ancient Egypt*. Oxford: Oxford University Press.
- Sowada KN. 2009. *Egypt in the Eastern Mediterranean during the Old Kingdom, An Archaeological Perspective*. Orbis Biblicus et Orientalis 237). Fribourg: Fribourg Academic Press.
- Stuiver M, Polach HA. 1977. Discussion: reporting of ¹⁴C data. *Radiocarbon* 19(3):355–63.
- van den Brink ECM, Levy TE. 2002. Interaction models, Egypt and the Canaanite periphery. In: van den Brink ECM, Levy TE, editors. *Egypt and the Levant, Interrelations from the 4th through the Early 3rd Millennium BCE*. London: Leicester University Press. p 3–38.
- Wenke RJ. 2009. *The Ancient Egyptian State, the Origins of Egyptian Culture (c.8000–2000 BC)*. Cambridge: Cambridge University Press.
- Yizhaq M, Mintz G, Cohen I, Khalaily H, Weiner S, Boaretto E. 2005. Quality controlled radiocarbon dating of bones and charcoal from the early Pre-Pottery Neolithic B (PPNB) of Motza (Israel). *Radiocarbon* 47(2):193–206.